LANGMUIR

Article

pubs.acs.org/Langmuir

Comparison of Zirconium Phosphonate-Modified Surfaces for Immobilizing Phosphopeptides and Phosphate-Tagged Proteins

Florian Forato,[†] Hao Liu,[‡] Roland Benoit,[§] Franck Fayon,[∥] Cathy Charlier,[⊥] Amina Fateh,[⊥] Alain Defontaine,[⊥] Charles Tellier,[⊥] Daniel R. Talham,[*,‡] Clémence Queffélec,[*,†] and Bruno Bujoli[†]

[†]Chimie et Interdisciplinarité: Synthèse Analyse Modélisation (CEISAM), Université de Nantes, CNRS, UMR 6230, 2 rue de la Houssinière, BP 92208, 44322 Nantes Cedex 3, France

[‡]Department of Chemistry, University of Florida, Gainesville, Florida 32611-7200, United States

[§]CRMD-CNRS, 1B rue de la férollerie, 45071 Orléans Cedex 2, France

[∥]CNRS, CEMHTI UPR3079, Université de Orléans, F-45071 Orléans, France

[⊥]Fonctionnalité et Ingénierie des Protéines (UFIP), Université de Nantes, CNRS, UMR 6286, 2 rue de la Houssinière BP 92208, 44322 Nantes Cedex 3, France

Supporting Information

ABSTRACT: Different routes for preparing zirconium phosphonate-modified surfaces for immobilizing biomolecular probes are compared. Two chemical-modification approaches were explored to form self-assembled monolayers on commercially available primary amine-functionalized slides, and the resulting surfaces were compared to well-characterized zirconium phosphonate monolayer-modified supports prepared using Langmuir−Blodgett methods. When using $POCl_3$ as the amine phosphorylating agent followed by treatment with zirconyl chloride, the result was not a zirconium-phosphonate monolayer, as commonly assumed in the literature, but rather the process gives adsorbed zirconium oxide/hydroxide species and to a lower extent adsorbed zirconium phosphate and/or phosphonate. Reactions giving rise to these products were modeled in homogeneous-phase studies. Nevertheless, each of the three modified surfaces effectively immobilized phosphopeptides and phosphopeptide tags fused to an affinity protein. Unexpectedly, the zirconium oxide/hydroxide modified surface, formed by treating the amine-coated slides with $POCl_3/Zr^{4+}$, afforded better immobilization of the peptides and proteins and efficient capture of their targets.

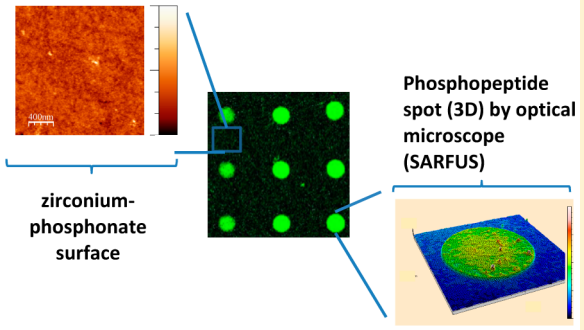

INTRODUCTION

Many methods have been developed for functionalizing material surfaces such as dip-coating, spin-coating,[1,2] self-assembled monolayers (SAMs),[3−8] layer-by-layer assembly,[9−12] vapor deposition,[13] Langmuir−Blodgett deposition,[1,14,15] and plasma treatment[16,17] for applications ranging from electronics to medical devices.[18−22] Depending on the nature of the surface to be modified, different functional groups can be employed to immobilize molecular, polymer, or biomolecular surface modifiers. To prepare useful devices, a strong binding between the probe and the support is required while using chemical processes that are simple and inexpensive but robust enough to ensure consistency in applications. Thus, the goal is to develop general methods for immobilizing peptides and proteins requiring few or no chemical modification of the probes and using easily accessible microarray substrates. Among these, phosphonic acids have emerged as a powerful tool to modify oxide and metal surfaces because the formation of P−O−metal ionocovalent bonds usually provides highly stable architectures, especially for metal cations in high oxidation states. Modifiers are normally added to protect or optimize the chemical nature of metal or metal oxide surfaces for the environment in which they will be employed, but the same immobilization chemistry can be used for the purpose of studying surface-confined molecules or biomolecules. For example, phosphate-bearing biological probes, including oligonucleotides, peptides, or small proteins,[23−28] have been shown to bind strongly to Zr^{4+}-modified surfaces, and the potential of these substrates for the design of biological microarrays was demonstrated in our groups.[23−26]

An effective surface for accepting phosphate-tagged molecules or biomolecules is a monolayer of Zr^{4+} ions bound to a phosphonic acid-terminated surface. Exceptionally smooth, well-defined zirconium phosphonate films can be prepared using Langmuir−Blodgett (LB) methods, and these surfaces have been usefully employed.[29] However, the large-scale production of such substrates at low cost is very unlikely because of the nature of the LB process. For this reason, in the

Received: March 16, 2016
Revised: May 9, 2016

DOI: 10.1021/acs.langmuir.6b01020
Langmuir XXXX, XXX, XXX−XXX

present study we compare the capture efficiency of proteins bearing phosphorylated peptide tags immobilized on zirconium phosphonate (ZrP) coatings made by different routes, including a self-assembly method commonly used in the literature and a novel approach utilizing a phosphonic acid bearing an *N*-hydroxysuccinimide derivative. The performance of the two chemical modification processes is compared to that of slides prepared using the LB process as a reference when immobilizing different phosphopeptides and affinity proteins. The phosphorylated peptides and proteins were found to specifically bind to each surface. The best performance was found for the primary-amine-coated slides treated first with $POCl_3$, followed by zirconyl chloride. Surprisingly, we show that this process does not result in a zirconium phosphonate monolayer, as is commonly assumed, but rather gave a mixed metal oxide/hydroxide layer. Nevertheless, this surface effectively immobilized the phosphate-modified peptides and proteins.

MATERIALS AND METHODS

Starting Materials. All commercially available reagents, including *N*,*N*′-disuccinimidyl carbonate, zirconyl chloride octahydrate, 2,4,6-collidine, phosphorus oxytrichloride ($POCl_3$), octadecyltrichlorosilane, α-casein, and HPLC-grade solvents were purchased from Aldrich. Reagents were of analytical grade and were used as received from commercial sources unless otherwise indicated. Glass slides were purchased from Goldseal (Horseshoe, NC) (3 in. × 1 in., thickness 0.93−1.05 mm). Aminopropylsilane glass slides (SuperAmine 2) were purchased from Arrayit (Sunnyvale, CA). Hydrophobic glass slides were made using octadecyltrichlorosilane following the method of Maoz and Sagiv.[30] The zirconium octadecylphosphonate Langmuir−Blodgett monolayers were prepared on the hydrophobic slides as described previously.[14,15] Phosphorylated biotinylated peptides (0P, 1P, 2P, 2P′, 3P, and 4P) were purchased from ProteoGenix (Schiltighem, France). The buffer used throughout the experiments consisted of 10 mM glycine, 10 mM TRIS base, 10 mM 2-(*N*-morpholino)ethanesulfonic acid(MES), and 10 mM acetic acid, which allows buffers to be prepared in the 2−10 pH range (pH 3, 7.4).

Preparation and Modification of Amine-Terminated Slides. SuperAmine 2 slides were used as received. For route A, the slides were soaked in a 1:1 solution of 2,4,6-collidine (20 mM) and $POCl_3$ (20 mM) in anhydrous acetonitrile and agitated for 16 h. For route B, they were soaked in a solution of a phosphonic acid bearing an *N*-hydroxysuccinimide end (compound **4**, 0.1 mM) and 4-dimethylaminopyridine (0.1 mM) in anhydrous dichloromethane and agitated for 24 h. The slides were rinsed with either acetonitrile (route A) or dichloromethane (route B) and annealed at 150 °C for 24 h to promote stable covalent bond formation. The phosphonate-terminated samples were then exposed to a 25 mM $ZrOCl_2{\cdot}8H_2O$ solution in Milli-Q water overnight. The slides were finally rinsed with Milli-Q water and stored under argon in Milli-Q water.

Production and Purification of Tagged Proteins. H4 Nanofitins are recombinant proteins derived from Sac7d from *Sulfolobus acidocaldarius* and evolved by ribosome display to bind lysozyme. The sequence of H4 Nanofitin was fused with the phosphorylatable tag (ARAEREDSDSSSEDE) containing four sites of phosphorylation in plasmid pQE30H4P.[28] The recombinant pQE30H4P1ala plasmid containing an H4 phosphorylatable tag (ARAEREDADAASEDE) with one serine was derived by site-directed mutagenesis from pQE30H4P.

For protein production, the BL21(DE3) *E. coli* strain transformed with these plasmids was cultivated in 1 L of Luria−Bertani (LB) medium containing ampicillin (100 μg/mL) at 37 °C until the optical density at 600 nm was 0.8. Isopropyl-1-β-D-thio-1-galactoside (IPTG) (1 mM) was added for induction, and cells were grown overnight at 30 °C. The proteins were first purified on Ni-NTA columns (QIAGEN) and then phosphorylated in vitro with recombinant α-casein kinase (CKII). The Nanofitins (100 μM) were incubated for 6 h at 30 °C in 50 mM Tris-HCl, 50 mM $MgCl_2$, 1 μg of α-CK2, 1 mM ATP, 2.5 mM DTT, 0.01% Triton X100, 10% glycerol, and 125 mM imidazole at pH 7.5, and the purification was completed by gel filtration on Superdex 75 (GE Healthcare).

Microarray Spotting and Incubation Conditions. The modified slides were washed once with ultrapure water and dried by centrifugation (1500 rpm, 1 min). The slides were then spotted with a noncontact spotter (sciFlexArrayer S3 piezo electric dispenser, Scienion). Spotting was performed inside a chamber at 25 °C and 60% humidity. The spotted slides were placed in an incubation chamber at 37 °C for 1 h. To passivate the unspotted areas, slides were treated after spotting with a solution of 0.3 wt % α-casein in a TBS (Tris-buffered saline) solution of TrisHCl (20 mM) and NaCl (150 mM) at pH 7.4. In the case of spotted biotinylated phosphopeptides, incubation was performed by applying an Alexa 647-labeled streptavidin solution (0.1 μg/mL in TBS-0.3% α-casein) to the substrate for 1 h at room temperature in the dark. In the case of the mono- or tetraphosphorylated tag fused to proteins, incubation was performed by applying an Alexa 647-labeled lyzozyme solution (0.1 μg/mL in TBS-0.3% α-casein) to the substrate for 1 h at room temperature in the dark. Microarrays were washed three times with TBS for 5 min and then once with ultrapure water. Finally, the slides were spun dry by centrifugation at 1500 rpm for 1 min. All washes and incubations were performed in small staining jars at room temperature on an oscillating shaker.

Microarray Analysis. All microarrays were scanned on a Scanarray Gx apparatus (PerkinElmer) with a laser power and gain value of 60. Suitable excitation wavelength and emission filters were used to detect Alexa 647:650 nm (excitation), 665 nm (emission). The location of each analyte spot on the array and the measurement of the fluorescence intensities was performed using the Genepix mapping software (Axon laboratories, Palo Alto, CA).

FT-IR. Vibrational spectroscopy data were obtained using a Bruker-Tensor 27 FT-IR spectrometer with the OPUS Data Collection Program for the analysis.

X-ray Photoelectron Spectrometry (XPS). The X-ray photoelectron spectroscopy (XPS) measurements were performed with a Thermo Scientific Escalab 250 using monochromatic Al Kα (1486.6 eV) radiation with a spot size of about 600 μm. The high-resolution spectra were collected with 20 eV pass energy at a takeoff angle of θ = 90°, and the C 1s peak position of 284.6 eV was used to calibrate the spectra. After Shirley background subtraction, XPS spectra were deconvoluted into Gaussian−Lorentzian components.

Time-of-Flight Secondary Ion Mass Spectrometry (ToF-SIMS). ToF-SIMS experiments were performed with a TOF.SIMS 5 instrument from ION-TOF GmbH using a 25 keV bismuth liquid metal ion gun (LMIG). The primary ion beam of 25 keV Bi^{3+} was operated in static mode with a primary pulsed beam current of 2.5 pA. Appropriate charge neutralization (20 eV electronic flood gun) was used to avoid charging of the samples during data collection. The detection was performed within a mass range of 1 to 800 amu. With a data acquisition of 100 s, the total fluence was less than 1012 ions/cm^2, ensuring static conditions. Depth chemical profile (perpendicular to the surface) and chemical imaging measurements were also performed.

Liquid-State NMR Spectroscopy. Liquid-state ^1H, ^{13}C, and ^{31}P spectra were recorded in deuterated solvents on a Bruker Avance apparatus operating at 300 or 400 MHz.

Solid-State NMR Spectroscopy. Solid-state magic-angle spinning (MAS) NMR experiments were performed on a Bruker Advance HD spectrometer operating at 17.6 T (^1H and ^{31}P Larmor frequencies of 750 and 303.6 MHz, respectively) using a 4 mm double-resonance MAS probe and a spinning frequency of 14 kHz. Quantitative ^{31}P single-pulse MAS spectra were acquired using a 20° flip angle (pulse duration of 1 μs) and a recycle delay of 40 s. The ^{31}P cross-polarization (CP) MAS spectra[31] were recorded using different contact times ranging from 0.25 to 12.5 ms and a recycle delay of 1 s. For all ^{31}P 1D MAS experiments, ^1H decoupling was achieved using the SPINAL64 sequence[32] with a radio frequency field strength of 50 kHz. 2D ^{31}P homonuclear CP-MAS correlation experiments were performed at a spinning frequency of 14 kHz with a contact time of 2.5 ms and a

DOI: 10.1021/acs.langmuir.6b01020
Langmuir XXXX, XXX, XXX−XXX

Scheme 1. Chemical Modifications of SuperAmine 2 Slides for the Preparation of Zirconium Phosphonate-Modified Surfaces

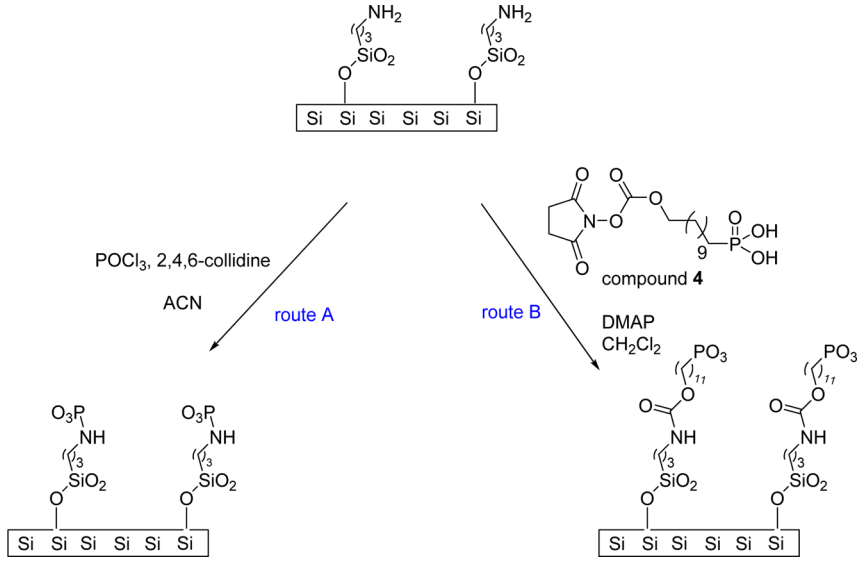

Scheme 2. Synthesis of Compound 4

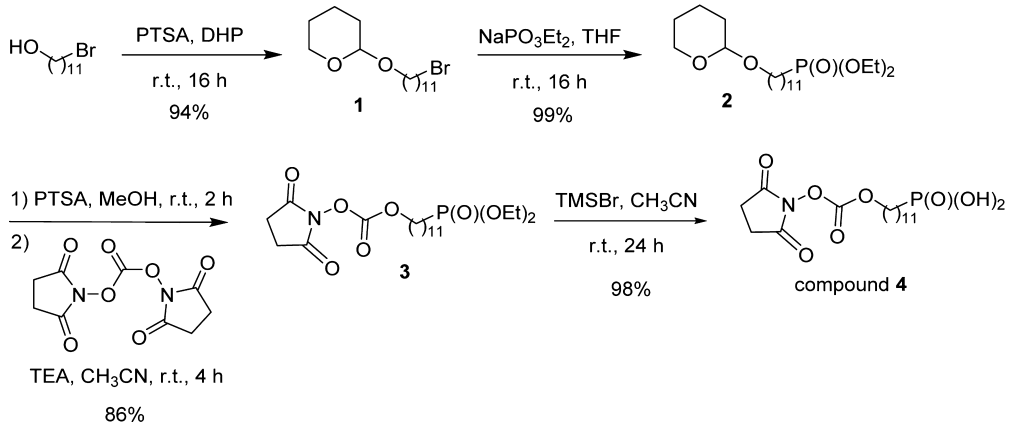

recycle delay of 1s. The RFDR[33] homonuclear dipolar recoupling pulse sequence was applied during the mixing time of the 2D experiment to promote magnetization transfer between neighboring ^{31}P atoms. ^{1}H SPINAL decoupling (50 kHz RF-field strength) was applied in both direct and indirect dimensions. ^{31}P chemical shifts were referenced relative to 85 wt % H_3PO_4.

Sarfus Measurements. Nanometer-scale optical images were obtained from a Sarfus 3D apparatus (Nanolane, Le Mans, France). For optical studies, this equipment included an upright optical microscope (DM4000, Leica Microsystems, Wetzlar, Germany) and specific contrast-enhanced substrates termed Surfs. For optical thickness measurements which are based on color/thickness correspondence, a calibration standard made of nanometric steps and image treatment software (Sarfusoft 2.0) were used.[34] The standard Surfs (top-layer SiO_2) were modified with amines by the company, and then the two procedures to form the zirconium phosphonate monolayer were applied.

RESULTS AND DISCUSSION

Preparation of Zirconium Phosphonate Surfaces. Along with the Langmuir−Blodgett method we described previously,[14,15] two other chemical modification methods for preparing Zr^{4+}-modified surfaces were investigated and compared (Scheme 1). The two chemical modification routes begin with primary amine-functionalized glass slides, which are easily available from commercial sources because they are classically used for the preparation of oligonucleotide microarrays.[35,36] In the present study, we used SuperAmine 2 slides (SA). Massari et al.[37] and Katz et al.[10,38] reported the phosphorylation of aminopropylsilane coatings on ITO or glass slides using $POCl_3$ treatment. A detailed characterization of the resulting zirconium phosphonate surface was not provided, although these surfaces were subsequently successfully used as self-assembled monolayer supports. This approach was studied on the SA slides and is described as route A in Scheme 1. An alternative route involving the reaction of the terminal NH_2 groups with a phosphonic acid bearing an *N*-hydroxysuccinimide derivative, compound **4**, was also considered (route B, Scheme 1). In both cases, the phosphonate-modified surface was then soaked in a $ZrOCl_2{\cdot}8H_2O$ solution overnight, which is generally found to be long enough to allow Zr^{4+} binding to the surface $-PO_3^{2-}$ groups.[39]

Compound **4** was obtained in four steps with a 78% overall yield, adapting a procedure described by Reetz et al. (Scheme 2).[40] First, 11-bromoundecanol was protected with a tetrahydropyranyl group to yield compound **1**. An Arbuzov reaction was then carried out using sodium hypophosphite to produce compound **2**. Removal of the THP protecting group and reaction with *N*,*N*′-disuccinimidyl carbonate led to compound **3**, which, after deprotection of the phosphonate

DOI: 10.1021/acs.langmuir.6b01020
Langmuir XXXX, XXX, XXX−XXX

esters with bromotrimethylsilane, yielded final compound **4** (more details in the SI).

Characterization of Zirconium Phosphonate Surfaces by XPS and ToF-SIMS Analysis. The phosphorus and zirconium contents of the coatings obtained by routes A and B were analyzed using XPS (Table 1 and Figure 1). For route A, the XPS spectrum of the slide after the $POCl_3$ treatment evidenced a P 2p peak at a binding energy (133.1 eV) expected for phosphorus in CPO_3 environnements,[41,42] indicating that the phosphorylation was successful. However, an analysis of the surface after subsequent treatment with Zr^{4+} (Table 1) showed only a small zirconium contribution, but no significant phosphorus peak could be detected. On the contrary, when compound **4** was used to modify the amine-functionalized slides (route B), the peak assigned to CPO_3 was detected even after the zirconation step (Table 1). In this case, the P/Zr ratio measured by XPS was 1.2, close to the expected value of 1 for complete zirconation of the phosphonate layer. For both routes, the Zr XPS signal appeared as a resolved spin doublet at $Zr(3d_{5/2})$ binding energies of 182.6 (route A) and 182.5 eV (route B), close to the values reported for zirconium oxide[43−45] and hydroxide[43] environments. The XPS analysis showed that the phosphorylation step worked well in both cases, but only route B led to the formation of the expected zirconium phosphonate monolayer after zirconium oxychloride treatment. For route A, the zirconium content and the P/Zr ratio measured by XPS were much weaker than expected, suggesting that a different reaction occurred, thus leading mainly to a Zr oxide/hydroxide deposit on the amine-functionalized slide, as shown below.

Table 1. XPS Analysis of Aminosilane-Coated Glass Slides Treated with $POCl_3/Zr^{4+}$ (Route A) or with Compound 4/Zr^{4+} (Route B)

		relative peak intensities (%)		
route	treatment	P 2p	Zr 3d	P/Zr ratio
A	$POCl_3$ (16 h)	1		
A	$POCl_3$ (16 h), then Zr^{4+}	trace	0.32	
B	compound **4** (16 h)	4.30		
B	compound **4** (16 h), then Zr^{4+}	2.9	2.39	1.2

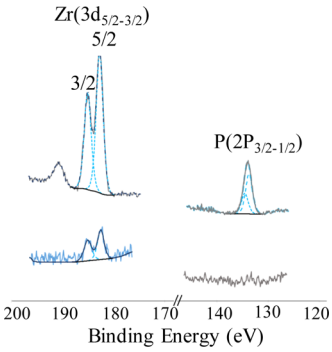

Figure 1. XPS Zr 3d and P 2p peaks of the zirconium phosphonate monolayer surfaces from route B (top) and from route A (bottom) after zirconium oxychloride treatment. The dashed lines correspond to fits to one Zr 3d and one P 2p spin doublet. Relative peak intensities are listed in Table 1.

Time-of-flight secondary ion mass spectroscopy (ToF-SIMS) is an effective tool for detecting P−O−M bonds, as shown by Menzel and co-workers[46] in the case of modified titanium, and was used here to characterize the surface reactions taking place for the two preparation methods. In the case of route B, PO_3Zr^-, PO_4Zr^-, $NHCOO^-$, $C_3H_{10}PO^-$, $C_3H_6NCO^-$, CH_3P^-, $C_2PO_3^-$, $C_2H_4PO_3^-$, and C_3N^- fragments were detected in negative ion mode with a bismuth cluster source (Bi_3) (Figure 2), thus confirming the expected surface modification. In contrast, the analysis revealed a smaller content of ZrO_2^- fragments and only very weak phosphorus-containing fragments following the zirconation step of route A, in agreement with the XPS results. A significant signal due to hydroxyl fragments was also detected. Together, XPS and ToF-SIMS indicated that route A does not result in the formation of a zirconium phosphonate layer. Furthermore, ToF-SIMS chemical mapping of SiO_2 negative fragments also revealed uncovered pristine zones of the glass slide surface, indicating that route A leads to a nonuniform deposit onto the surface.

The homogeneity of the coating obtained from route B was mapped, and the ionic profile of the surface deposit was

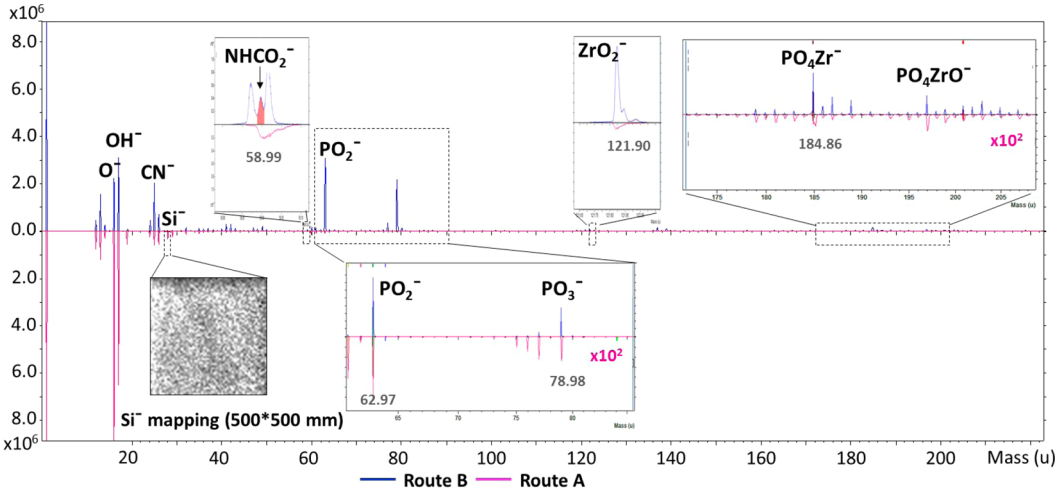

Figure 2. ToF-SIMS spectra of the zirconium phosphonate surface obtained according to route A (pink) and route B (blue) after zirconium oxychloride treatment. Regions of $NHCO_2^-$, PO_2^-, PO_3^-, ZrO_2^-, PO_4Zr^-, and PO_4ZrO^- fragments are expanded. The chemical mapping of SiO_2 negative fragments on slides prepared following route A is shown in the inset.

DOI: 10.1021/acs.langmuir.6b01020
Langmuir XXXX, XXX, XXX−XXX

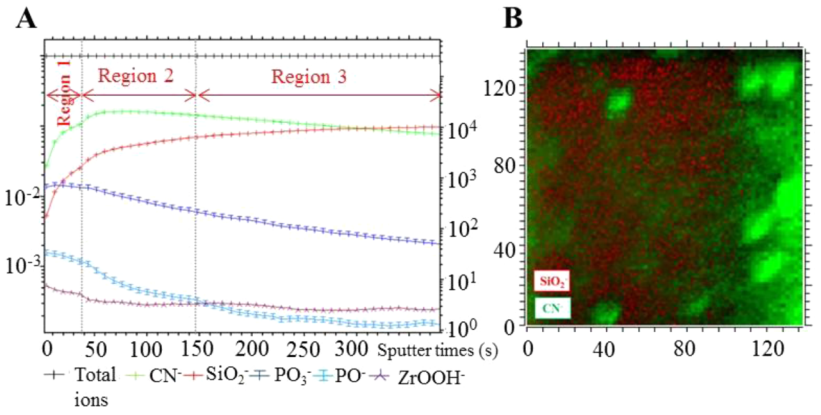

Figure 3. (A) ToF-SIMS negative ion profile of the layer obtained from route B. Regions 1 to 3 are described in the text. (B) Overlap of the maps of the SiO_2^- and CN^- ionic chemical fragments.

recorded (Figure 3). The top of the layer (region 1 in Figure 3) showed fragments of zirconium oxide/hydroxide and phosphorus-containing PO_3^- or PO_2^- groups coming from the zirconium phosphonate layer. Deeper into the layer (region 2), CN^- fragments increase and reach a maximum whereas the fragments of zirconium oxide/hydroxide and phosphorus decrease. Finally, all of the elements forming the zirconium phosphonate monolayer as well as the primary amine layer decrease, and SiO_2^- from the glass substrate increases (region 3). Chemical mapping of the area studied by ionic etching was also performed. The intensity of the CN^- negative fragments, which were found to exhibit an efficient ionization cross-section, was used as a chemical tracer of the surface coverage. As shown in Figure 3B, this analysis reveals a nonuniform coverage of the slide surface with the formation of aggregates on the scale of tens of micrometers.

Evaluating the Surface Reaction in the Homogeneous Phase. Our observations related to route A contradict assumptions from the literature,[10,37,38] although a detailed surface chemical analysis of the zirconium phosphonate surface expected at the end of the process has never been demonstrated. To rationalize our results, a similar reaction was conducted in solution, using butylamine as a model for the primary amine-functionalized slide. After reaction for 16 h with phosphoryl chloride and 2,4,6-collidine in acetonitrile at room temperature under nitrogen, the mixture was evaporated and ^1H and ^{31}P spectra were recorded (Figures S2–S4). The ^1H NMR spectra confirmed the quantitative formation of $CH_3(CH_2)_2CH_2NHP(O)Cl_2$ because the resonance assigned to the CH_2 bound to nitrogen showed an upfield shift of 0.5 ppm and a multiplicity characteristic of coupling with the phosphorus atom (doublet of triplets with $^2J_{HN}$ and $^3J_{HP}$ coupling constants of 14 and 7 Hz, respectively). This assignment is confirmed by recording the ^1H spectrum with ^{31}P decoupling for which this resonance appeared as a triplet. Similarly, the ^1H-decoupled ^{31}P NMR spectrum showed a major peak at around 15 ppm that gave rise to a quadruplet ($^3J_{HP}$ = 14 Hz) when turning off ^1H decoupling, thus confirming N–P bond formation. In the next step, the addition of a $ZrOCl_2{\cdot}8H_2O$ water solution (25 mM, 100 mL)) to $CH_3(CH_2)_3NHP(O)Cl_2$ (10 mmol) resulted in the formation of a white precipitate after a few minutes, which was recovered by filtration following 16 h of stirring.

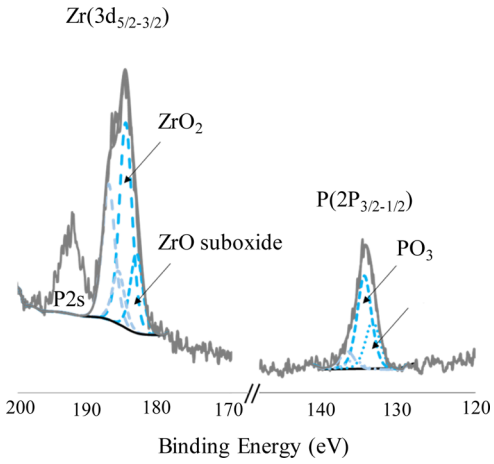

Figure 4. XPS Zr 3d and P 2p peaks obtained for the white solid formed by the reaction of $CH_3(CH_2)_3NHP(O)Cl_2$ with a zirconium oxychloride solution. The dashed lines show the fits with two Zr and two P spin doublets, and the arrows indicate the two contributions.

According to ^1H NMR, the evaporated filtrate showed the presence of butylamine as the only product. The white solid precipitate was first characterized by XPS (Figure 4), showing the presence of phosphorus and zirconium with a P/Zr atomic ratio of 2.5, and nitrogen was present only in trace amounts. Line-shape analysis of the Zr 3d peak indicates the presence of two spin-doublet contributions, with relative intensities of ca. 1:3 and binding energies (183.4 and 184.9 eV) close to those reported for zirconium suboxide and ZrO_2.[45,47] The P 2p peak was also fitted with two contributions at 133.1 and 135.4 eV with relative intensities in a 1:4 ratio. These values are in the binding energy ranges reported for CPO_3, PO_4, HPO_4, and H_2PO_4 units.[48,49] As there is essentially no nitrogen in the XPS spectrum, it can be concluded that no zirconium phosphonate is present, and these two peaks likely correspond to PO_4 and H_2PO_4/HPO_4 environments. This assignment is consistent with the broad absorption in the FT-IR spectrum at 960–1250 cm^{-1}, characteristic of phosphate groups (Figure S5). Although the resolution of the spectrum was poor because of the amorphous character of this solid, it showed some similarities with the FT-IR spectrum of α-zirconium phosphate.[50]

To improve the structural description of this solid, solid-state MAS NMR experiments were performed. The ^{31}P MAS and CP-MAS spectra recorded at high magnetic field are shown in Figure 5A. These spectra exhibit an intense resonance at about −21 ppm with an asymmetric line shape indicating the

DOI: 10.1021/acs.langmuir.6b01020
Langmuir XXXX, XXX, XXX–XXX

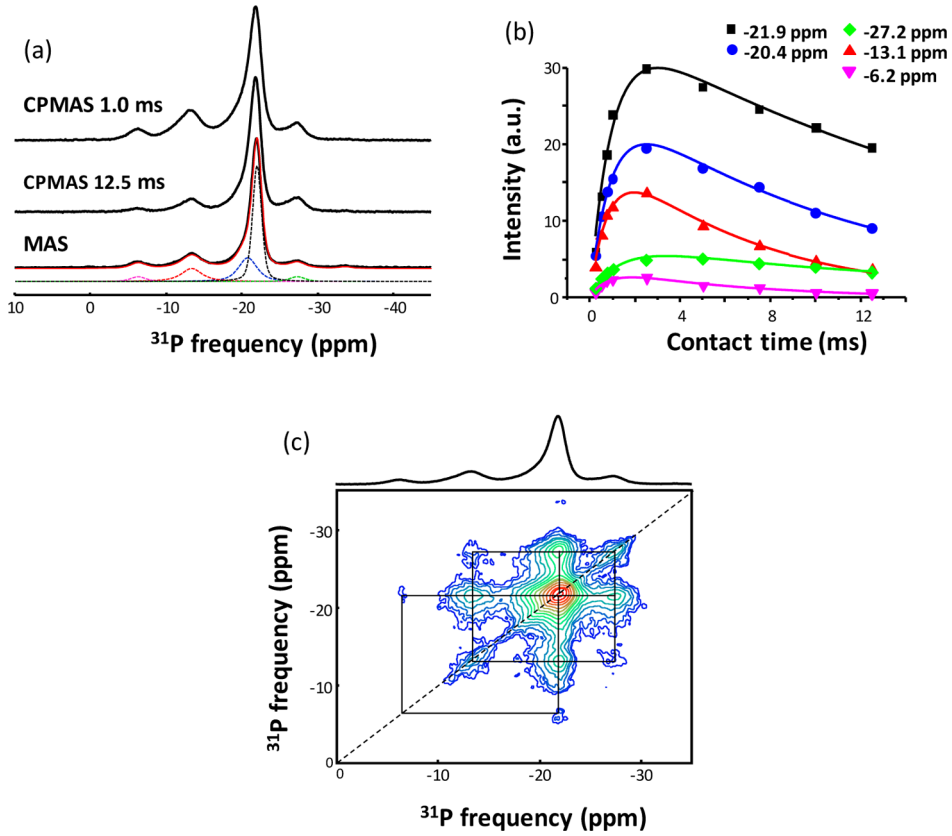

Figure 5. (a) ^{31}P CP (top, middle) and quantitative (bottom) MAS spectra of the white solid formed by the reaction of $CH_3(CH_2)_3NHP(O)Cl_2$ with a zirconium oxychloride solution (B_0 = 17.6 T, spinning frequency of 14 kHz MAS, CP contact times of 2.5 (top) and 12.5 (middle) ms). (b) Variation of the intensities of the different ^{31}P resonances as a function of the CP time. Experimental values (symbols) were fitted to the classical model[56] (lines), assuming that the ^{31}P longitudinal relaxation time in the rotating frame ($T_{1\rho P}$) is much longer than the ^{31}P−^{1}H cross-relaxation time T_{PH}. The expression $I(t) = I_0\left(1 - \frac{T_{PH}}{T_{1\rho H}}\right)^{-1}\left(e^{-t/T_{1\rho H}} - e^{-t/T_{PH}}\right)$ was used, where $T_{1\rho H}$ is the ^{1}H longitudinal relaxation time in the rotating frame.[56,57] (c) 2D ^{31}P homonuclear magnetization exchange CP-MAS spectrum obtained at 17.6 T using the RFDR dipolar recoupling sequence (mixing time of 40 ms, spinning frequency of 14 kHz). Cross-correlation peaks are indicated by the black lines, and the diagonal of the spectrum is indicated by the dashed line.

presence of two overlapping contributions (at −21.9 and −20.4 ppm) and additional resolved resonances of weaker intensities. Most of the observed ^{31}P isotropic chemical shifts (Table S1) are similar to those reported for layered α- and γ-zirconium phosphates,[51−53] and the overlapping contributions (−21.9 and −20.4 ppm) and the peaks at −13.1 and −27.2 ppm were assigned to HPO_4, H_2PO_4, and PO_4 units of a zirconium phosphate framework, respectively. An almost constant shift of ∼7 ppm between these peaks was observed, and following this chemical shift trend, the remaining resonance at −6.2 ppm was assigned to H_3PO_4 units. ^{31}P CP-MAS spectra recorded at low spinning frequency also indicated a weak chemical shift anisotropy (<20 ppm) ruling out the presence of a phosphonate environment.[54] It should be noted that, in addition to these main lines, a peak of very weak intensity (<0.5%) at a chemical shift (−33.6 ppm) characteristic of pyrophosphate units[55] was also observed. The assignment is also consistent with the CP time constants (T_{PH}) determined from the intensity variations of each individual resonance as a function of the CP time (Figure 5B). Similar T_{PH} values of 0.95 and 0.92 ms were found for the peaks at −21.9 and −20.4 ppm (HPO_4 groups). In contrast, the resonances of H_2PO_4 and H_3PO_4 units with stronger P−H dipolar interactions exhibited shorter T_{PH} values of 0.82 and 0.84 ms, while a longer T_{PH} of 1.2 ms was found for the PO_4 resonance (with weaker P−H dipolar couplings). The observation of these relatively broad resonances therefore revealed the presence of disordered layered zirconium phosphate frameworks. To investigate the possible presence of different zirconium phosphate phases in the sample, 2D ^{31}P magnetization exchange MAS NMR spectra were recorded using the RFDR recoupling sequence. In this experiment, the polarization transfer in the mixing time is driven by the homonuclear dipolar interaction, allowing long-range interatomic proximities to be probed at long mixing times. As shown in Figure 5C, the 2D exchange MAS spectrum obtained with a mixing time of 40 ms showed cross-correlation peaks among all of the individual resonances displayed in the 1D MAS spectrum, reflecting their short- and long-range spatial proximities, indicating that the sample contained a single phase. Therefore, NMR clearly reveals that the precipitate formed upon reacting the $RNHP(O)Cl_2$ with zirconium oxychloride is a disordered, hydrated layered zirconium phosphate phase made of HPO_4, H_2PO_4, and PO_4 units with adsorbed and/or intercalated H_3PO_4 molecules.

It is known in the literature that at low pH,[58−62] phosphoramidic acids are quickly hydrolyzed to release the corresponding amine and phosphoric acid, and the conclusion from the homogeneous phase reaction is that this phenomenon

DOI: 10.1021/acs.langmuir.6b01020
Langmuir XXXX, XXX, XXX−XXX

is expected to occur in the presence of a Zr^{4+} solution, which is very acidic (pH ~2). Our results thus suggest that even though N−P bond formation proceeds well in the surface reaction via phosphorylation of the amino end-groups of the slides using phosphoryl chloride, cleavage of this bond occurs during subsequent treatment with zirconium oxychloride. In the homogeneous phase reaction with $CH_3(CH_2)_3NHP(O)Cl_2$, a disordered layered zirconium phosphate phase precipitates. In the case of the aminosilane-coated slide treated with $POCl_3$, a similar reaction is expected to occur, with the excess zirconium being adsorbed onto the slide surface as zirconium oxide/hydroxide species. The resulting coating then consists mainly of an amorphous zirconium oxide/hydroxide layer with some adsorbed zirconium phosphate/hydrogenophosphate groups. This finding is consistent with related observations of Zr^{4+} hydrolysis. Mallouk[63] observed while working on the synthesis and exfoliation of zirconium phosphates that hydrolysis on the edges of the colloidal sheets of α-Zr−P can lead to the formation of a zirconium-rich three-dimensional material and that the ultimate product of the hydrolysis is small hydrated zirconium oxide particles. Tulock et al.[64] demonstrated that the hydrolysis of zirconium tetramers in aqueous solution will lead to the formation of zirconium oligomers and a decrease in pH even though hydrolysis will proceed slowly at room temperature. Interestingly, even though hydrolysis occurs at the surface, it is still very active as a support for adsorbing phosphorylated molecules,[39] peptides, and proteins, as will be shown below.

Peptide Spotting Experiments. The aminosilane-coated glass slides modified according to routes A and B were first compared to the previously studied zirconium phosphonate LB slides[14,15,25−27] for their ability to bind phosphorylated peptide anchors in a specific manner.[39] Five commercially available phosphorylated peptides and one nonphosphorylated peptide were used (Table 2), the same series studied in a previous report,[39] with each biotinylated on the C-terminal end to allow quantification of the immobilized probes upon incubation with streptavidin labeled with a fluorophore (Alexa Fluor 647).

Table 2. Peptide Sequences Used for the Binding Study with Zirconium Phosphonate-Modified Substrates

name	peptides
0P	Biotin-REEDSDSDSEDE
1P	Biotin-REEDEDDD-pS-EDE
2P	Biotin-REED-pS-DDD-pS-EDE
2P′	Biotin-REEDEDD-pS-pS-EDE
3P	Biotin-REED-pS-DD-pS-pS-EDE
4P	Biotin-REED-pS-D-pS-pS-pS-EDE

Solutions of the six peptides were spotted on the different slides using a concentration of 10 μM in buffer at two different pH values (3 and 7.4). After spotting, a blocking step with α-casein was applied, which provides efficient saturation of the nonspotted areas because of its high phosphate content, thus preventing nonspecific protein binding.[26]

As shown previously,[39] the nonphosphorylated peptide binds very poorly at neutral and acidic pH, whatever the nature of the modified surfaces. On the other hand, the binding of phosphopeptides 1P to 4P was sensitive to the pH value. At pH 7.4 (Figure S7), weak fluorescence intensities could be measured after incubation with labeled streptavidin, indicating relatively poor immobilization on the three types of surfaces. At pH 3, strong binding was observed for the phosphorylated peptides. As observed earlier, the binding of 2P′ is especially effective, for which a 6-fold increase in fluorescence intensity was observed compared to that of the other phosphorylated peptides (Figure 6).[39]

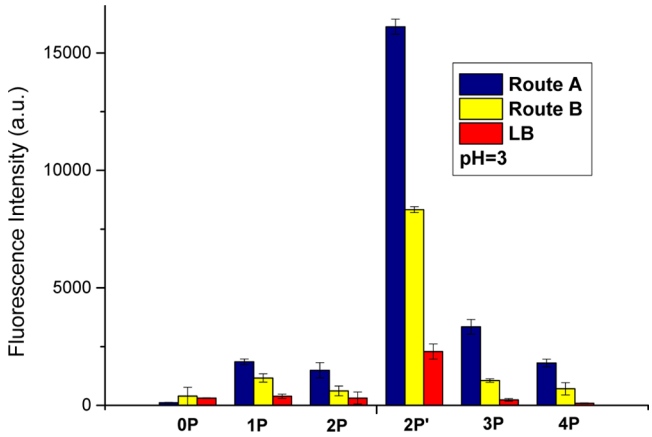

Figure 6. Fluorescence analysis of zirconium phosphonate substrates spotted with biotinylated peptide sequences containing zero (0P), one (1P), two (2P and 2P′), three (3P), or four (4P) phosphorylated serine groups at pH 3 (spotting concentration: 10 μM). Three substrates were spotted: zirconium phosphonate LB films (noted as LB) and aminosilane-coated glass slides modified according to route A (noted as SA, $POCl_3$, and Zr) or route B (noted as SA, compound **4**, Zr). After spotting, saturation, and rinsing, the substrates were incubated with Alexa Fluor 647-labeled streptavidin.

To investigate whether immobilization of the phosphorylated peptide proceeds via the expected formation of Zr^{4+}-OPO_3-peptide linkages, the same experiments were performed on (i) the unmodified aminosilane-coated glass slides, (ii) the aminosilane slides treated only with $POCl_3$, or (iii) the aminosilane slides treated only with zirconium oxychloride. In the first two cases, no binding was observed, whereas for the aminosilane-coated slides treated with zirconium oxychloride, some binding of the peptides could be observed, although with a very low intensity compared to that of LB-derivatized zirconium phosphonate films or slides prepared according to routes A and B.

Optical Imaging of Peptide Spotting. The Sarfus technique was used to record optical images of the peptides bound to the surface after incubation with Alexa Fluor 647-labeled streptavidin. This technology is based on an optical microscope working in reflected differential interference contrast mode together with nonreflecting substrates termed "surfs" that increase the sensitivity of a traditional microscope by up to 2 orders of magnitude,[34] allowing the direct visualization of nanoscale structures with a vertical resolution of less than 1 nm. Phosphorylated peptides were deposited at pH 3 on primary amine-terminated surfs modified according to route A, and the optical thickness of the spots was measured after incubation with Alexa Fluor 647-labeled streptavidin (Figure 7).

The 2D and 3D visualizations of the spots obtained in the case of peptide 4P are shown in Figure 7A,B, respectively. The mean height is about 7 nm relative to the nonspotted areas, with a well-defined spot (Figure 7C). The same experiment was performed with peptide 4P at pH 3 on primary amine-terminated surfs modified according to route B. In this case

DOI: 10.1021/acs.langmuir.6b01020
Langmuir XXXX, XXX, XXX−XXX

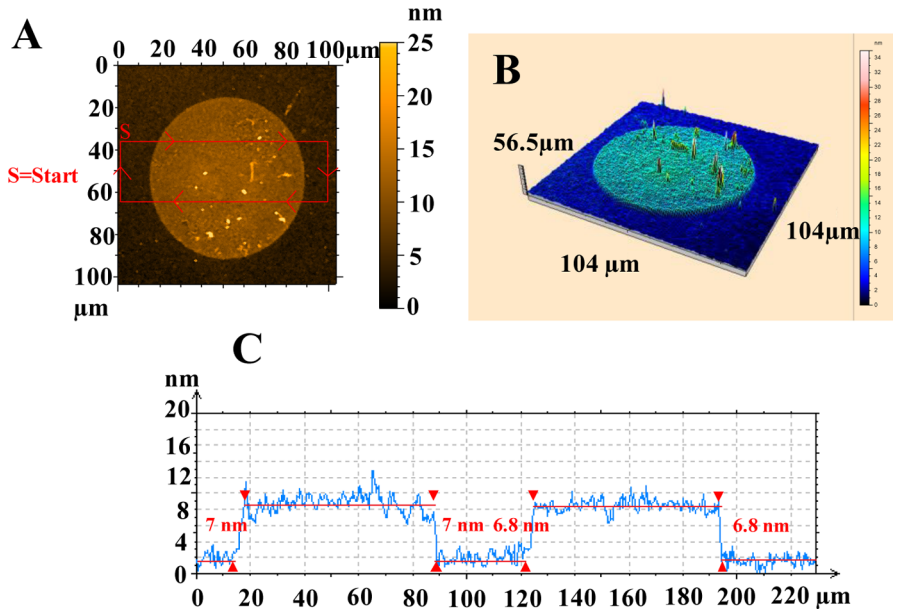

Figure 7. Sarfus image of a spot of phosphopeptide 4P at pH 3 (10 μM) on amine-terminated surfs modified according to route A. Spotting was performed using the noncontact spotter used for the microarray experiments, following saturation and rinsing, the substrates were incubated with Alexa Fluor 647-labeled streptavidin. (A) Microsocope image at 5× magnification. (B) 3D Sarfus representation of the spot. (C) Extracted profile giving the optical thickness of the spot along the red line shown in A. The mean height is about 7 nm.

(Figure S7), the spot was poorly defined with a nonregular optical thickness, which was difficult to measure. This observation is consistent with results from Figure 6, confirming again the better performance of primary amine-terminated slides modified according to route A, even though this surface does not consist of a zirconium phosphonate monolayer. The increase in peptide binding is most likely a consequence of the imperfect zirconium oxide/hydroxide coating giving rise to a greater surface area compared to that of the relatively smooth LB or self-assembled molecular monolayers.

Protein Immobilization. Finally, the last step was to compare how proteins bearing a phosphorylated peptide tag bind to the different supports. For these studies, we used as a model protein H4 Nanofitin, which specifically binds lysozyme and was engineered with different phosphate tags.[28,39] The immobilization was performed at pH 3 (Figure 8) and 7.4 (Figure S8), and the casein blocking and rinsing steps were performed at pH 7.4. As shown in Figure 7, no matter the nature of the support, immobilization of the protein was very effective at pH 3 when the fused tag had four phosphate binding sites, yielding significant target capture. The immobilization was also very effective at pH 7.4 (Figure S9) for the protein bearing four phosphate groups. When a single phosphate group is present on the peptide tag, contrary to the case of short peptides, the affinity of the phosphate group for the substrate is not strong enough to be preponderant over nonspecific and reversible binding of the protein, such as via carboxylic acid residues. It can be concluded that each of the three types of substrates investigated in this study can provide specific binding of phosphorylated peptide or protein probes.

CONCLUDING REMARKS

Zirconium phosphonate or zirconium phosphate coordinate-covalent binding is strong and chemically specific and has been shown to be a promising strategy for immobilizing appropriately functionalized peptides or proteins. Two chemical modification strategies for preparing Zr^{4+}-modified supports

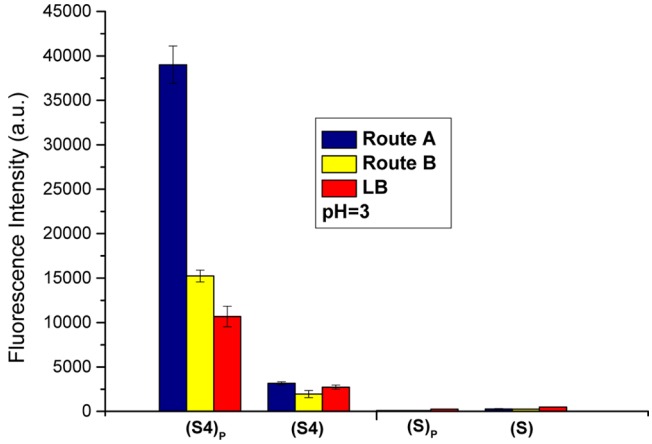

Figure 8. Fluorescence analysis of zirconium phosphonate substrates spotted with nonphosphorylated nanoffitins, S and S4, directed against lysozyme, and their phosphorylated analogues bearing one phosphate group, S_p, and four phosphate groups, $S4_p$, at pH 3 (spotting concentration 10 μM). Three substrates were spotted: zirconium phosphonate LB films (noted as LB) and aminosilane-coated glass slides modified according to route A (noted as SA, $POCl_3$, and Zr) or route B (noted as SA, compound **4**, Zr). After spotting, saturation, and rinsing, the substrates were incubated with Alexa Fluor 647-labeled lysozyme.

starting from primary amine-functionalized slides were compared to slides modified with an idealized monolayer, formed using the Langmuir−Blodgett method and previously shown to be effective. All three surfaces specifically bound short phosphorylated peptides or proteins bearing a phosphorylated peptide tag, especially at pH 3. Surprisingly, the widely used approach of preparing zirconated slides by treating primary-amine-functionalized glass slides with $POCl_3$ followed by zirconyl chloride did not generate a zirconium phosphonate monolayer as had been previously assumed but rather resulted in a nonuniform zirconium oxide/hydroxide-rich coating, likely

DOI: 10.1021/acs.langmuir.6b01020
Langmuir XXXX, XXX, XXX−XXX

in addition to some adsorbed zirconium phosphate species. Nevertheless, compared to the better-defined zirconium phosphonate monolayer-modified slides, this surface performed best when subsequently adsorbing phosphate-tagged peptides or proteins. The amorphous zirconium oxide/hydroxide coating remains very active toward phosphate, and increased surface area from the nonideal coating leads to larger extents of peptide or protein adsorption. This result opens new perspectives for developing surfaces functionalized with biological probes because the preparation of these substrates is simple and has a reasonable cost, making it potentially attractive for large-scale production.

■ ASSOCIATED CONTENT

Supporting Information

The Supporting Information is available free of charge on the ACS Publications website at DOI: 10.1021/acs.langmuir.6b01020.

Synthesis of compound A. ^{1}H and ^{31}P NMR of the experiments done in solution. FT-IR of the solid. ^{31}P isotropic chemical shifts of zirconium phosphonates and zirconium phosphates. Fluorescence intensity quantification for phosphopeptides and nonphosphorylated proteins and phosphorylated protein. Sarfus image of a spot of phosphopeptide 4P at pH 3 on amine-terminated surfs modified by a zirconium phosphonate monolayer obtained according to route B. (PDF)

■ AUTHOR INFORMATION

Corresponding Authors

*E-mail: talham@chem.ufl.edu.

*E-mail: Clemence.Queffelec@univ-nantes.fr.

Funding

The authors acknowledge financial support from the Centre National de la Recherche Scientifique and the U.S. National Science Foundation, Division of Chemistry under grant no. 0957155 (cofunded by the MPS/CHE and the Office of International Science and Engineering).

Notes

The authors declare no competing financial interest.

■ ACKNOWLEDGMENTS

We thank the Biogenouest IMPACT Academic Platform, Nantes, France, for the protein microarray analysis and are most grateful to the Genomics Platform of Nantes (Biogenouest Genomics) core facility for technical support.

■ REFERENCES

(1) Agina, E. V.; Usov, I. A.; Borshchev, O. V.; Wang, J. B.; Mourran, A.; Shcherbina, M. A.; Bakirov, A. V.; Grigorian, S.; Moller, M.; Chvalun, S. N.; Ponomarenko, S. A. Formation of Self-Assembled Organosilicon-Functionalized Quinquethiophene Monolayers by Fast Processing Techniques. *Langmuir* **2012**, *28* (46), 16186−16195.

(2) Shimomura, A.; Nishino, T.; Maruyama, T. Display of Amino Groups on Substrate Surfaces by Simple Dip-Coating of Methacrylate-Based Polymers and Its Application to DNA Immobilization. *Langmuir* **2013**, *29* (3), 932−938.

(3) Flink, S.; van Veggel, F.; Reinhoudt, D. N. Functionalization of Self-Assembled Monolayers on Glass and Oxidized Silicon Wafers by Surface Reactions. *J. Phys. Org. Chem.* **2001**, *14* (7), 407−415.

(4) Han, X.; Sun, S.; He, T. Preparation and Photolithography of Self-Assembled Monolayers of 10-Mercaptodecanylphosphonic Acid on Glass Mediated by Zirconium for Protein Patterning. *Colloids Surf., B* **2013**, *108*, 66−71.

(5) Love, J. C.; Estroff, L. A.; Kriebel, J. K.; Nuzzo, R. G.; Whitesides, G. M. Self-Assembled Monolayers of Thiolates on Metals as a Form of Nanotechnology. *Chem. Rev.* **2005**, *105* (4), 1103−1169.

(6) San Juan, R. R.; Allan, C. J.; Iqbal, M.; Eichhorn, S. H.; Macdonald, C. L. B.; Carmichael, T. B. New Dihexadecyldithiophosphate SAMs on Gold Provide Insight into the Unusual Dependence of Adsorbate Chelation on Substrate Morphology in SAMs of Dialkyldithiophosphinic Acids. *J. Am. Chem. Soc.* **2013**, *135* (42), 15784−15793.

(7) Wang, X. J.; Lieberman, M. Zirconium-Phosphonate Monolayers with Embedded Disulfide Bonds. *Langmuir* **2003**, *19* (18), 7346−7353.

(8) Yan, C.; Zharnikov, M.; Golzhauser, A.; Grunze, M. Preparation and Characterization of Self-Assembled Monolayers on Indium Tin Oxide. *Langmuir* **2000**, *16* (15), 6208−6215.

(9) Decher, G. Fuzzy Nanoassemblies: Toward Layered Polymeric Multicomposites. *Science* **1997**, *277* (5330), 1232−1237.

(10) Katz, H. E.; Schilling, M. L.; Chidsey, C. E. D.; Putvinski, T. M.; Hutton, R. S. Quaterthiophenediphosphonic Acid (Qdp) - A Rigid, Electron-Rich Building Block for Zirconium-Based Multilayers. *Chem. Mater.* **1991**, *3* (4), 699−703.

(11) Lee, H.; Kepley, L. J.; Hong, H. G.; Akhter, S.; Mallouk, T. E. Adsorption of Ordered Zirconium Phosphonate Multilayer Films on Silicon and Gold Surfaces. *J. Phys. Chem.* **1988**, *92* (9), 2597−2601.

(12) Lee, H.; Kepley, L. J.; Hong, H. G.; Mallouk, T. E. Inorganic Analogs of Langmuir-Blodgett Films - Adsorption of Ordered Zirconium 1,10-Decanebisphosphonate Multilayers on Silicon Surfaces. *J. Am. Chem. Soc.* **1988**, *110* (2), 618−620.

(13) Cao, Y.; Galoppini, E.; Reyes, P. I.; Duan, Z. Q.; Lu, Y. C. Morphology Effects on the Biofunctionalization of Nanostructured ZnO. *Langmuir* **2012**, *28* (21), 7947−7951.

(14) Byrd, H.; Pike, J. K.; Talham, D. R. Inorganic Monolayers Formed at an Organic Template - A Langmuir-Blodgett Route to Monolayer and Multilayer Films of Zirconium Octadecylphosphonate. *Chem. Mater.* **1993**, *5* (5), 709−715.

(15) Byrd, H.; Pike, J. K.; Talham, D. R. Extended-Lattice Langmuir-Blodgett-Films - Manganese Octadecylphosphonate Langmuir-Blodgett-Films Are Structural and Magnetic Analogs of Solid-State Manganese Phosphonates. *J. Am. Chem. Soc.* **1994**, *116* (17), 7903−7904.

(16) Denes, F. S.; Manolache, S. Macromolecular Plasma-Chemistry: An Emerging Field of Polymer Science. *Prog. Polym. Sci.* **2004**, *29* (8), 815−885.

(17) Recek, N.; Mozetic, M.; Jaganjac, M.; Milkovic, L.; Zarkovic, N.; Vesel, A. Adsorption of Proteins and Cell Adhesion to Plasma Treated Polymer Substrates. *Int. J. Polym. Mater.* **2014**, *63* (13), 685−691.

(18) Queffelec, C.; Petit, M.; Janvier, P.; Knight, D. A.; Bujoli, B. Surface Modification Using Phosphonic Acids and Esters. *Chem. Rev.* **2012**, *112* (7), 3777−3807.

(19) Zhang, G.-Y.; Deng, S.-Y.; Cai, W.-R.; Cosnier, S.; Zhang, X.-J.; Shan, D. Magnetic Zirconium Hexacyanoferrate(II) Nanoparticle as Tracing Tag for Electrochemical DNA Assay. *Anal. Chem.* **2015**, *87* (17), 9093−9100.

(20) Khassanov, A.; Steinrueck, H.-G.; Schmaltz, T.; Magerl, A.; Halik, M. Structural Investigations of Self-Assembled Mono Layers for Organic Electronics: Results from X-Ray Reflectivity. *Acc. Chem. Res.* **2015**, *48* (7), 1901−1908.

(21) Zhao, S.; Chen, Y.; Liu, B.; Chen, M.; Mao, J.; He, H.; Zhao, Y.; Huang, N.; Wan, G. A Dual-Task Design of Corrosion-Controlling and Osteo-Compatible Hexamethylenediaminetetrakis- (Methylene Phosphonic Acid) (HDTMPA) Coating on Magnesium for Biodegradable Bone Implants Application. *J. Biomed. Mater. Res., Part A* **2015**, *103* (5), 1640−1652.

(22) Guasch, J.; Conings, B.; Neubauer, S.; Rechenmacher, F.; Ende, K.; Rolli, C. G.; Kappel, C.; Schaufler, V.; Micoulet, A.; Kessler, H.; Boyen, H. G.; Cavalcanti-Adam, E. A.; Spatz, J. P. Segregation Versus Colocalization: Orthogonally Functionalized Binary Micropatterned

DOI: 10.1021/acs.langmuir.6b01020
Langmuir XXXX, XXX, XXX−XXX

Substrates Regulate the Molecular Distribution in Focal Adhesions. *Adv. Mater.* **2015**, *27* (25), 3737−3747.
(23) Lane, S. M.; Monot, J.; Petit, M.; Tellier, C.; Bujoli, B.; Talham, D. R. Poly(dG) Spacers Lead to Increased Surface Coverage of DNA Probes: An XPS Study of Oligonucleotide Binding to Zirconium Phosphonate Modified Surfaces. *Langmuir* **2008**, *24* (14), 7394−7399.
(24) Lane, S. M.; Monot, J.; Petit, M.; Bujoli, B.; Talham, D. R. XPS Investigation of DNA Binding to Zirconium-Phosphonate Surfaces. *Colloids Surf., B* **2007**, *58* (1), 34−38.
(25) Nonglaton, G.; Benitez, I. O.; Guisle, I.; Pipelier, M.; Leger, J.; Dubreuil, D.; Tellier, C.; Talham, D. R.; Bujoli, B. New Approach to Oligonucleotide Microarrays Using Zirconium Phosphonate-Modified Surfaces. *J. Am. Chem. Soc.* **2004**, *126* (5), 1497−1502.
(26) Monot, J.; Petit, M.; Lane, S. M.; Guisle, I.; Leger, J.; Tellier, C.; Talham, D. R.; Bujoli, B. Towards Zirconium Phosphonate-Based Microarrays for Probing DNA-Protein Interactions: Critical Influence of the Location of the Probe Anchoring Groups. *J. Am. Chem. Soc.* **2008**, *130* (19), 6243−6251.
(27) Cinier, M.; Petit, M.; Williams, M. N.; Fabre, R. M.; Pecorari, F.; Talham, D. R.; Bujoli, B.; Tellier, C. Bisphosphonate Adaptors for Specific Protein Binding on Zirconium Phosphonate-Based Microarrays. *Bioconjugate Chem.* **2009**, *20* (12), 2270−2277.
(28) Cinier, M.; Petit, M.; Pecorari, F.; Talham, D. R.; Bujoli, B.; Tellier, C. Engineering of a Phosphorylatable Tag for Specific Protein Binding on Zirconium Phosphonate Based Microarrays. *JBIC, J. Biol. Inorg. Chem.* **2012**, *17* (3), 399−407.
(29) Fabre, R. M.; Okeyo, G. O.; Talham, D. R. Supported Lipid Bilayers at Skeletonized Surfaces for the Study of Transmembrane Proteins. *Langmuir* **2012**, *28* (5), 2835−2841.
(30) Maoz, R.; Sagiv, J. On the Formation and Structure of Self-Assembling Monolayers. 1. A Comparative ATR-Wetability Study of Langmuir-Blodgett and Adsorbed Films on Flat Substrates and Glass Microbeads. *J. Colloid Interface Sci.* **1984**, *100* (2), 465−496.
(31) Pawsey, S.; McCormick, M.; De Paul, S.; Graf, R.; Lee, Y. S.; Reven, L.; Spiess, H. W. H-1 Fast MAS NMR Studies of Hydrogen-Bonding Interactions in Self-Assembled Monolayers. *J. Am. Chem. Soc.* **2003**, *125* (14), 4174−4184.
(32) Fung, B. M.; Khitrin, A. K.; Ermolaev, K. An Improved Broadband Decoupling Sequence for Liquid Crystals and Solids. *J. Magn. Reson.* **2000**, *142* (1), 97−101.
(33) Bennett, A. E.; Griffin, R. G.; Ok, J. H.; Vega, S. Chemical Shift Correlation Spectroscopy in Rotating Solids: Radio Frequency-driven Dipolar Recoupling and Longitudinal Exchange. *J. Chem. Phys.* **1992**, *96* (11), 8624−8627.
(34) Ausserré, D.; Valignat, M.-P. Wide-Field Optical Imaging of Surface Nanostructures. *Nano Lett.* **2006**, *6* (7), 1384−1388.
(35) Fixe, F.; Dufva, M.; Telleman, P.; Christensen, C. B. V. Functionalization of Poly(methyl Methacrylate) (PMMA) as a Substrate for DNA Microarrays. *Nucleic Acids Res.* **2004**, *32*, e9.
(36) Pack, S. P.; Kamisetty, N. K.; Nonogawa, M.; Devarayapalli, K. C.; Ohtani, K.; Yamada, K.; Yoshida, Y.; Kodaki, T.; Makino, K. Direct Immobilization of DNA Oligomers onto the Amine-Functionalized Glass Surface for DNA Microarray Fabrication Through the Activation-Free Reaction of Oxanine. *Nucleic Acids Res.* **2007**, *35*, e110.
(37) Massari, A. M.; Gurney, R. W.; Wightman, M. D.; Huang, C. H. K.; Nguyen, S. B. T.; Hupp, J. T. Ultrathin Micropatterned Porphyrin Films Assembled via Zirconium Phosphonate Chemistry. *Polyhedron* **2003**, *22* (22), 3065−3072.
(38) Katz, H. E.; Schilling, M. L. Electrical-Properties of Multilayers Based on Zirconium-Phosphate Phosphonate Bonds. *Chem. Mater.* **1993**, *5* (8), 1162−1166.
(39) Liu, H.; Queffelec, C.; Charlier, C.; Defontaine, A.; Fateh, A.; Tellier, C.; Talham, D. R.; Bujoli, B. Design and Optimization of a Phosphopeptide Anchor for Specific Immobilization of a Capture Protein on Zirconium Phosphonate Modified Supports. *Langmuir* **2014**, *30* (46), 13949−13955.
(40) Reetz, M. T.; Ruggeberg, C. J.; Droge, M. J.; Quax, W. J. Immobilization of Chiral Enzyme Inhibitors on Solid Supports by Amide-Forming Coupling and Olefin Metathesis. *Tetrahedron* **2002**, *58* (42), 8465−8473.
(41) Bomben, K. D.; Moulder, J. F.; Sobol, P. E.; Stickle, W. F. *Handbook of X-ray Photoelectron Spectroscopy. A Reference Book of Standard Spectra for Identification and Interpretation of XPS Data*; Physical Electronics: Eden Prairie, MN, 1995.
(42) Wu, X. X.; Radovic, L. R. Inhibition of Catalytic Oxidation of Carbon/carbon Composites by Phosphorus. *Carbon* **2006**, *44* (1), 141−151.
(43) Barr, T. Esca Study of Termination of Passivation of Elemental Metals. *J. Phys. Chem.* **1978**, *82* (16), 1801−1810.
(44) Nefedov, V.; Gati, D.; Dzhurinskii, B.; Sergushin, N.; Salyn, Y. X-Ray Electron Study of Oxides of Elements. *Zh. Neorg. Khim.* **1975**, *20* (9), 2307−2314.
(45) Okazaki, Y.; Tateishi, T.; Ito, Y. Corrosion Resistance of Implant Alloys in Pseudo Physiological Solution and Role of Alloying Elements in Passive Films. *Mater. Trans., JIM* **1997**, *38* (1), 78−84.
(46) Adden, N.; Gamble, L. J.; Castner, D. G.; Hoffmann, A.; Gross, G.; Menzel, H. Phosphonic Acid Monolayers for Binding of Bioactive Molecules to Titanium Surfaces. *Langmuir* **2006**, *22* (19), 8197−8204.
(47) Bensch, W.; Helmer, O.; Muhler, M.; Ebert, H.; Knecht, M. Experimental and Theoretical Band-Structure of the Layer Compound Zrsite. *J. Phys. Chem.* **1995**, *99* (10), 3326−3330.
(48) Castle, J. E. In *Practical Surface Analysis by Auger and X-ray Photoelectron Spectroscopy*; Briggs, D., Seah, M. P., Eds.; John Wiley and Sons: Chichester, 1983. Castle, J. E. *Surf. Interface Anal.* **1984**, *6*, 302.
(49) Moretti, G. X-ray Photoelectron and Auger Electron Spectroscopy. In *Handbook of Heterogeneous Catalysis*; Wiley-VCH Verlag GmbH & Co. KGaA, 2008.
(50) Horsley, S. E.; Nowell, D. V.; Stewart, D. T. Infrared and Raman-Spectra of Alpha-Zirconium Phosphate. *Spectrochim. Acta Part -Mol. Biomol. Spectrosc.* **1974**, *A-30* (2), 535−541.
(51) Clayden, N. Solid-State Nuclear-Magnetic-Resonance Spectroscopic Study of Gamma-Zirconium Phosphate. *J. Chem. Soc., Dalton Trans.* **1987**, 1877−1881.
(52) Odobel, F.; Bujoli, B.; Massiot, D. Zirconium Phosphorate Frameworks Covalently Pillared with a Bipyridine Moiety. *Chem. Mater.* **2001**, *13* (1), 163−173.
(53) Maclachlan, D.; Morgan, K. P-31 Solid-State Nmr-Studies of the Structure of Amine-Intercalated Alpha-Zirconium Phosphate - Reaction of Alpha-Zirconium Phosphate with Excess Amine. *J. Phys. Chem.* **1990**, *94* (19), 7656−7661.
(54) Burwell, D.; Valentine, K.; Thompson, M. P-31 and C-13 Chemical-Shift Tensors in Zirconium Phosphonates. *J. Magn. Reson.* **1992**, *97* (3), 498−510.
(55) King, I. J.; Fayon, F.; Massiot, D.; Harris, R. K.; Evans, J. S. O. A Space Group Assignment of ZrP_2O_7 Obtained by P-31 Solid State NMR. *Chem. Commun.* **2001**, No. No. 18, 1766−1767.
(56) Sternhell, S., Mehring, M. *Principles of High Resolution NMR in Solids*; Springer-Verlag, Berlin, Heidelberg, NY, 1983. Sternhell, S. M. *Org. Magn. Reson.* **1983**, *21*, 770.
(57) Kolodziejski, W.; Klinowski, J. Kinetics of Cross-Polarization in Solid-State NMR: A Guide for Chemists. *Chem. Rev.* **2002**, *102* (3), 613−628.
(58) Bondarenko, N. A.; Kharlamov, A. V.; Vendilo, A. G. Synthesis of Nonsymmetrical Dialkylamines on the Basis of Diphenylphosphinic Amides. *Russ. Chem. Bull.* **2009**, *58* (9), 1872−1885.
(59) Halmann, M.; Samuel, D.; Lapidot, A. Mechanism of Hydrolysis of Phosphoramidic Acid. *J. Chem. Soc.* **1963**, 1299.
(60) Hanson, E. L.; Schwartz, J.; Nickel, B.; Koch, N.; Danisman, M. F. Bonding Self-Assembled, Compact Organophosphonate Monolayers to the Native Oxide Surface of Silicon. *J. Am. Chem. Soc.* **2003**, *125* (51), 16074−16080.
(61) Lonnberg, T.; Ora, M.; Lonnberg, H. Hydrolytic Reactions of Nucleoside Phosphoramidates: Kinetics and Mechanisms. *Mini-Rev. Org. Chem.* **2010**, *7* (1), 33−43.
(62) Maiti, M.; Michielssens, S.; Dyubankova, N.; Maiti, M.; Lescrinier, E.; Ceulemans, A.; Herdewijn, P. Influence of the

DOI: 10.1021/acs.langmuir.6b01020
Langmuir XXXX, XXX, XXX−XXX

Nucleobase and Anchimeric Assistance of the Carboxyl Acid Groups in the Hydrolysis of Amino Acid Nucleoside Phosphoramidates. *Chem. - Eur. J.* **2012**, *18* (3), 857−868.
(63) Kaschak, D. M.; Johnson, S. A.; Hooks, D. E.; Kim, H. N.; Ward, M. D.; Mallouk, T. E. Chemistry on the Edge: A Microscopic Analysis of the Intercalation, Exfoliation, Edge Functionalization, and Monolayer Surface Tiling Reactions of Alpha-Zirconium Phosphate. *J. Am. Chem. Soc.* **1998**, *120* (42), 10887−10894.
(64) Tulock, J. J.; Blanchard, G. J. Investigating Hydrolytic Polymerization of Aqueous Zirconium Ions Using the Fluorescent Probe Pyrenecarboxylic Acid. *J. Phys. Chem. B* **2002**, *106* (14), 3568−3575.

DOI: 10.1021/acs.langmuir.6b01020
Langmuir XXXX, XXX, XXX−XXX